# ANALYSIS OF THE J INTEGRAL DURING THE DUCTILE FRACTURE OF STEEL AND ALUMINIUM COMPACT TENSION SPECIMENS

RAM B. BHAGAT and MICHAEL B. HOUSE

*The Pennsylvania State University*
*227 Hammond Building, University Park, PA 16802*

## ABSTRACT

A two-dimensional nonlinear finite element analysis on compact tension specimens of HY-130 and HY-140 steel, and 7075 aluminum has been carried out to determine the effects of plasticity on the *J*-integral and strain energy density fracture criterion. The computed values of the *J*-integral for compact tension specimens of steel and aluminum alloys ($0.533 \leq a/W \leq 0.884$) remain path independent up to a certain load which is attributed to crack initiation, and then diverge. There is a unique signature of the strain energy density *(dW/dV)* ahead of the crack in the 0° direction: the strain energy density first decreases, reaches a minimum and then increases with increasing distance from the crack tip. The minimum strain energy density shows a unique dependence on the applied load. This leads to the prediction of the fracture loads for the cracked specimens, which is comparable to fracture loads predicted by the *J*-integral.

## KEYWORDS

Strain energy density, *J*-integral, ductile fracture, compact tension specimens, *PAPST*, nonlinear finite element analysis.

## INTRODUCTION

The *J*-integral, formulated as a possible fracture criterion has been used in materials which exhibit nonlinear stress-strain behavior. The *J*-integral has been shown to accurately predict crack initiation in structural alloys (Begley and Landes, 1972; Hutchinson, 1968, 1983) and has been studied numerically as it applies to limited crack extension (Sorensen, 1979; Dean and Hutchinson, 1980; Brocks and Yuan, 1989; Jun et al., 1991). The need for a ductile fracture criterion stems from the inherent plasticity that surrounds a crack tip prior to crack growth in metals and alloys. Linear elastic fracture mechanics (LEFM) analysis requires small scale yielding, therefore elastic-plastic fracture mechanics (EPFM) must be employed when the crack tip plastic zone (CTPZ) is relatively large. Fracture parameters such as the crack tip opening displacement (CTOD) and analytical solutions of the slip-line field have been studied as they relate to ductile instability and have met with some success (McClintock, 1971). From the work of Hutchinson (1968), Rice and Rosengren (1968), the stresses, strains, and displacements are known within a radius representing the size of the plastic zone in the case of large scale and general yielding for linear hardening elastic-plastic materials. This zone is called the HRR zone (attributed to Hutchinson, Rice and Rosengren), while the material outside the crack tip plastic zone remains in the elastic region. The work of Hutchinson, Rice and Rosengren gained recognition due to the variety of problems that could be described by the HRR zone located near a loaded crack tip in ductile metals.

As noted by Orowan (1950), the stress necessary to fracture ductile, tough metals is much greater than the stress required for brittle material fracture, and is accounted for through an additional plastic deformation work term, $\gamma_p$. This deformation is absorbed through a process of microvoid nucleation, growth and linking. Microscopically these voids may begin to form in individual grains at stresses much lower than the yield point. Depending upon the material's strain hardening, void nucleation and growth may occur homogeneously in areas of high dislocation densities or may occur heterogeneously along grain boundaries or particle inclusions (Goods and Brown, 1979). These micromechanisms contribute to significant plasticity, requiring criteria such as the *J*-integral to characterize the crack tip process zone.

In the past, the path independence of the *J*-integral has been established, excluding contours that pass through dissimilar media, holes or drastic dimensional changes or where a large amount of crack extension takes place (Vanderglas, 1990). It has been shown analytically that the *J*-dominated HRR region is valid up to 0.25 times the length of the plastic zone radius (McMeeking and Parks, 1979; McMeeking, 1977; Shih and German, 1981; Needleman and Tvergaard, 1983). Thus the *J*-integral has been used to study fracture problems involving crack tip plasticity beyond the scope of LEFM (Schmitt and Kienzler, 1989).

Another fracture criterion which may be used to characterize the onset of instability in ductile fracture involves the strain energy density concept. Bhagat et al. (1989) have proposed that their numerical analysis leads to the following parameters: (a) a critical load satisfying the necessary and sufficient conditions for the initiation of crack growth, (b) a crack length dependent energy parameter, and (c) a material characteristic energy parameter corresponding to global instability which leads to fracture. Their work on A-517 steel suggests that the material characteristic energy parameter may be considered as a measure of fracture toughness in ductile metals.

In the present investigation, a detailed non-linear finite element analysis has been carried out on a variety of structural alloys to compare the strain energy density based fracture criterion to that of the *J*-integral in HY-130 steel and 7075 aluminum. The compact tension specimens of interest conform with ASTM standards for the toughness testing of ductile materials. The effects of plasticity upon the numerically calculated values of the *J*-integral will also be discussed.

## NUMERICAL ANALYSIS

The Computer Program *PAPST*. The finite element code, *PAPST*, (**P**lastic-**A**xisymmetric/**P**lanar **S**tructures) used in this analysis has been developed by the Navy over the last several years to study fracture in elastic-plastic solids (Hilton and Gifford, 1983). Listed below are the capabilities and modifications that have been made to the *PAPST* code. The execution procedure and additional postprocessors have been documented to account for all the modifications. The origins of the *PAPST* program can be traced back to another finite element code, *APES*, which was limited to linear elastic fracture problems (Gifford, 1975). Gifford and Nash subsequently modified this code to accept nonlinear material characteristics and have published their findings on crack problems in elastic-plastic materials (Hilton and Gifford, 1983). To handle the mathematical instability at the crack tip, a special enriched mode I singularity element was incorporated with 8x8 Gaussian quadrature. Away from the highly stressed regions, *PAPST* uses 12-noded isoparametric quadrilateral 2-D elements with 4x4 Gaussian quadrature. All of the nodes are located on the perimeter of the element. These elements allow stresses to vary over the face of the element thus requiring fewer elements to model a given structure. Both element types are capable of handling linear hardening materials such as those studied by Hutchinson (1968), Rice and Rosengren (1968). A comparison to constant stress (strain) triangular elements is given in the *APES* manual (Gifford, 1975) showing the accuracy of using these enhanced elements.



Solutions are obtained nonlinearly using the Newton-Raphson iteration technique. The nonlinear capability of *PAPST* incorporates the $J_2$-incremental flow theory of plasticity and the von Mises yield criteria. The *PAPST* code approximates the true stress-strain curve of a material using either multilinear or Ramberg-Osgood power hardening approximations. *PAPST* is capable of modeling either purely kinematic or isotropic hardening materials or may model a mixture of the two. *PAPST* handles both plane stress and plane strain conditions. The *J*-integral, an important parameter in nonlinear fracture mechanics, as discussed earlier, may be calculated over 10 paths surrounding the crack tip.

Materials. Two types of steel (HY-130 and HY-140) as well as 7075 aluminum have been investigated. The compact tension specimens which have been analyzed conform to current ASTM standards, see Table 1.

Table 1. Compact tension specimen geometry and material data (Hilton and Gifford, 1983; Metals Handbook, 1985)

| Material | *W* (mm) | *B* (mm) | *a* (mm) | *a*/*W* | $\sigma_y$ (MPa) |
|---|---|---|---|---|---|
| HY-130 | 50.8 | 25.4 | 39.04 | 0.7685 | 896.3 |
| | 50.8 | 25.4 | 41.22 | 0.8115 | |
| | 50.8 | 25.4 | 42.92 | 0.8843 | |
| HY-140 | 50.8 | 25.4 | 39.04 | 0.7685 | 965.3 |
| 7075 Al | 50.8 | 25.4 | 39.04 | 0.7685 | 413.7 |
| | 50.8 | 25.4 | 41.22 | 0.8115 | |

Multilinear material modeling of the true stress strain curves are used to represent all the materials as is shown in Fig. 1.

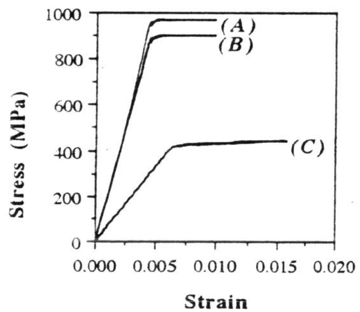


Figure 1. Stress-strain curves of HY-140 steel ***(A)***, HY-130 steel ***(B)*** and 7075 aluminum ***(C)***.

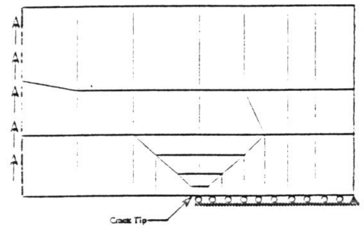


Figure 2. Representation of upper half of compact tension specimen showing appropriate boundary conditions.

Modeling of Compact Tension Specimens. One half of each specimen was modeled due to geometric symmetry as can be seen in Fig. 2. The relatively small number of incorporated elements is due to the higher order elements which allow stresses and strains to vary cubically across the element face. The nodes along the ligament are constrained to move only in the horizontal direction while the outer edge corner node is fixed to prevent free body translation or rotation. A uniform shear stress is applied to the left edge.

## RESULTS AND DISCUSSION

Due to the ductile nature of steel and aluminum we were interested in the crack tip plastic zone (CTPZ) and its dependence on the crack length. *J*-integral values were established on several different paths in both steel and aluminum specimens and the relative path independence of the *J*-integral will be demonstrated. The strain energy parameters $(dW/dV)_{min}$ and $(dW/dV)^*_{min}$ presented by Bhagat et al. (1989) were verified and will be discussed at length. Finally, stress and strain contour plots are presented to study how the stresses are distributed in front of the crack tip.

Material Deformation. A plot of a typical deformed mesh of 7075 aluminum is shown in Fig. 3. The applied load is 27234 N, corresponding to the loading conditions at a critical value of the strain energy density, which will be discussed at length later. The *J*-integral paths are located as shown. Similar plots were obtained for HY-140 steel and HY-130 steel.

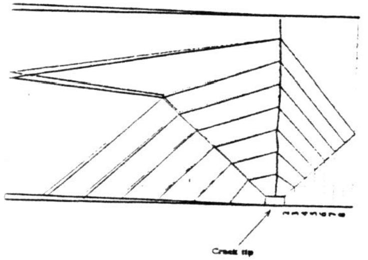


Figure 3. Picture showing the deformed upper half of a compact tension specimen model constructed of 7075 aluminum. The crack tip ($a/W$=0.7685) is located as shown.

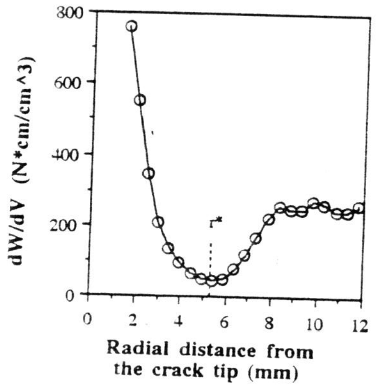


Figure 4. Strain energy density plotted against the radial distance from the crack tip in HY-130 steel ($a/W$=0.7685).

Strain Energy Density. The strain energy density $(dW/dV)$ in front of the crack tip was calculated using *PAPST*. At a critical radius the strain energy density dropped to a minimum value designated $(dW/dV)_{min}$ as is shown in Fig. 4. Earlier studies have shown that this "U-shaped" signature is found in the $\Theta=0°$ direction ahead of the crack tip (Bhagat et al., 1989). These values of $(dW/dV)_{min}$ were plotted against the applied load and at a critical load, the values of $dW/dV$ began to decrease as is shown in Fig. 5. This peak value of the strain energy density signifies the point at which the structure begins to expend energy in the form of crack growth. The maximum value of $(dW/dV)_{min}$ is denoted as $(dW/dV)^*_{min}$.

A range of crack length to width ratios ($0.7685 \leq a/W \leq 0.8843$) were numerically analyzed upon HY-130 steel, while two crack length to width ratios ($a/W$=0.7685 and $a/W$=0.8115) were analyzed upon 7075 aluminum. For the cases in which the numerical solutions produced a sharp peak in $(dW/dV)_{min}$, the failure load could be approximated by extrapolating the curve to



intersect the load axis (see Fig. 5). For example, in HY-130 steel with $a/W$=0.8115, the extrapolated curve intersects the load axis at 18683 N, and when $a/W$=0.8843, the predicted failure load is approximately 6450 N. The above method of failure load prediction is self consistent. The fracture loads of the aluminum specimens are less than those observed in the steel, while larger crack lengths sustain lower fracture loads than the smaller crack lengths, as expected.

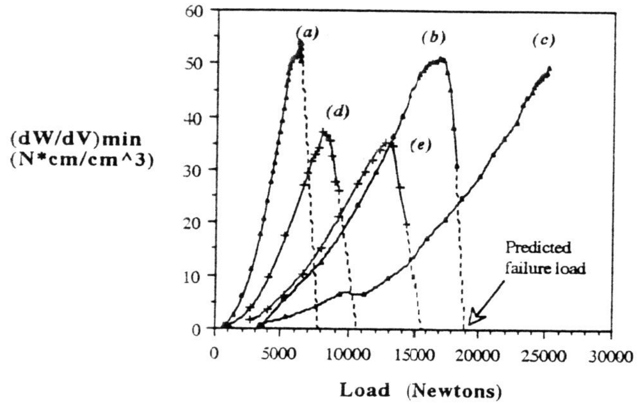


Figure 5. $(dW/dV)_{min}$ plotted against applied load for three crack lengths in HY-130 steel ($a/W$=0.7685, 0.8115 and 0.8843) and two crack lengths in 7075 aluminum ($a/W$=0.7685 and 0.8115). Fracture load is determined by extrapolating curve to the load axis.

Crack Tip Plasticity. Figures 6a and 6b present the effective stress distribution at the critical load, $P^*$, required for $(dW/dV)^*_{min}$ in HY-130 steel and 7075 aluminum ($a/W$=0.8115). These critical loads are 16868 N and 7909 N for the steel and aluminum specimens, respectively. Note that the yielded zone in the steel specimen is confined to a region near the free edge, while the CTPZ in the aluminum is present along the majority of ligament length. The difference in the size of the yielded regions may be attributed to the variation in stiffness between the two materials. Similar results were obtained for a range of crack lengths ($0.7685 \leq a/W \leq 0.8843$) under the identical loading conditions. The size of the yielded regions about the crack tip were found to decrease with increasing crack length, as expected.

Even though all the majority of the *J*-integral contour paths in 7075 aluminum (as shown in Fig. 6a) pass through the CTPZ at $P^*$, the variation from the averaged value of the *J*-integral is only 3%. However, when the load is increased to 1.13P* the variation from the average *J*-integral value increases to 7%. Figure 8 illustrates how the *J*-integral varies along the crack ligament in 7075 aluminum ($a/W$=0.7685) for load increments from $0.21P^*$ to $1.13P^*$. Similar trends can be observed in HY-130 as shown in Figs. 9 and 10.

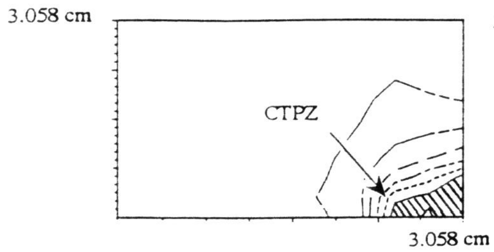


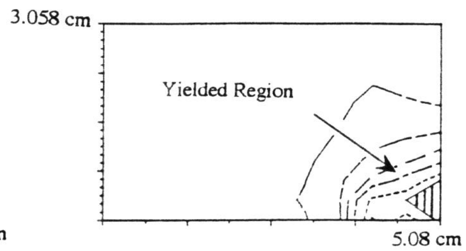


Figure 6a. Contour plot of the von Mises effective stress in 7075 aluminum showing the CTPZ. ($a/W$=0.8115)

Figure 6b. Contour plot of the von Mises effective stress in HY-130 steel showing the CTPZ. ($a/W$=0.0.8115)

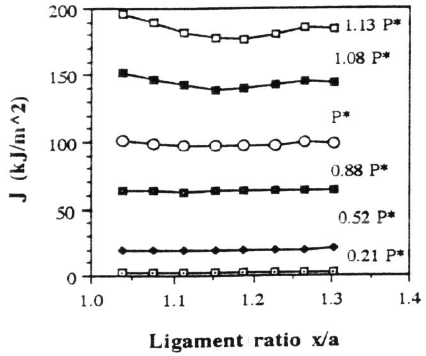


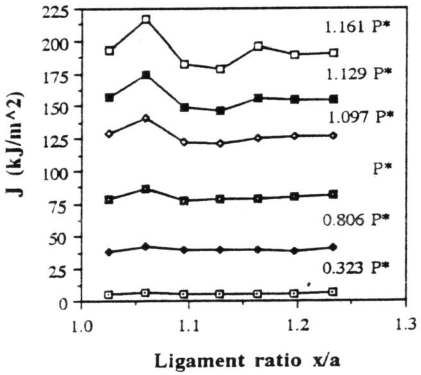


Figure 7. Variation of $J$ along the crack tip ligament for 7075 aluminum ($a/W$=0.7685). Note the variation of $J$ is small until the load is increased beyond $P^*$.

Figure 8. Variation of $J$ along the crack tip ligament for 7075 aluminum ($a/W$=0.8115). Note the variation of $J$ is small until the load is increased beyond $P^*$.



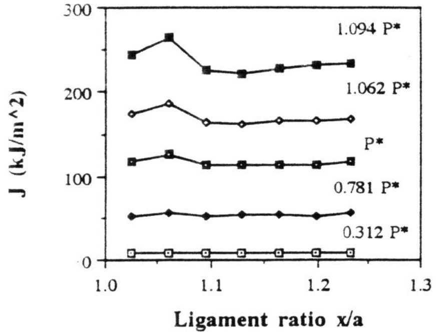


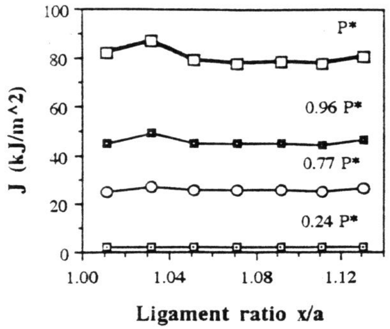


Figure 9. Variation of $J$ along the crack tip ligament for HY-130 steel ($a/W$=0.8115). Note the variation of $J$ is small until the load is increased beyond $P^*$.

Figure 10. Variation of $J$ along the crack tip ligament for HY-130 steel ($a/W$=0.8843). Note the variation of $J$ is small until the load is increased beyond $P^*$.

The crack initiation load may be predicted by studying the variation of the $J$-integral as a function of applied load. Typically these plots exhibit asymptotic behavior, approaching a critical value of $P$. This information can then be used to predict the critical loading state of a cracked structure. The work of Gifford (1978) has been verified in this investigation through the plot shown in Fig 12. To establish the validity of the strain energy density based fracture criterion, the predicted values of the failure loads were compared to the failure loads determined using the $J$-integral. Figure 13 indicates the asymptotic behavior of the $J$-integral and shows the corresponding fracture load predicted using the strain energy density concept (refer to Fig. 5). The results are comparable to within 15% from the values predicted by the $J$-integral.

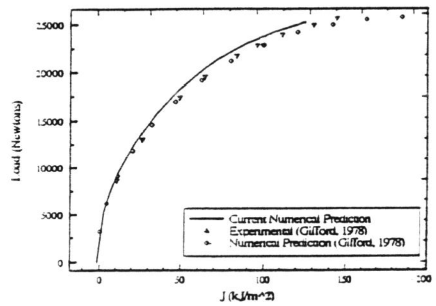


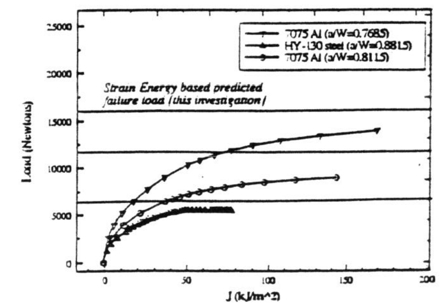


Figure 12. Plots of the $J$-integral for HY-130 steel (a/W=0.7685) showing comparison to the work of Gifford (1978).

Figure 13. Plots of the $J$-integral for HY-130 steel and 7075 aluminum comparing the $J$-integral fracture criterion to the strain energy density criterion

## SUMMARY AND CONCLUSIONS

A series of materials have been evaluated numerically for their fracture behavior and response to applied loads. Monolithic HY-130 steel, HY-140 steel and 7075 aluminum have been studied using *PAPST*, a nonlinear finite element package. In the case of HY-130 steel and 7075 aluminum, the strain energy distribution allows estimates of the crack initiation loads and the failure load to be made to within 15% of the failure loads predicted by the *J*-integral. The effect of crack tip plasticity and crack tip unloading on the *J*-integral have been established. Values of the *J*-integral were examined for a range of crack to width ratios ($0.533 \le a/W \le 0.884$) leading from small scale to extensive plasticity. When the loads were increased above a critical load (which is attributed to crack initiation), values of the *J*-integral deviated from the averaged value across the ligament of the specimens, up to 13%.

## REFERENCES


Begley, J.A. and Landes, J.D. [1972]. The J-integral as a Fracture Criterion. In: *Fracture Toughness, Proceedings of the 1971 National Symposium on Fracture Mechanics, Part II, ASTM STP 514*, (pp. 1-20) Philadelphia: American Society for Testing and Materials.

Bhagat, R.B., Amateau, M.F. and Crocken, M.L. [1989]. Non-Linear Finite Element Analysis of Cracked A-517 Steel Compact Tension Specimens. In: *Proceedings of the 7th International Conference on Fracture*, [Eds. K. Salama, K. Ravi-Chandar, D.M.R. Taplin and P. Rama Rao] 285-297.

Brocks, W. and Yuan, H. [1989]. Numerical Investigation on the Significance of *J* for Large Stable Crack Growth. *Engineering Fracture Mechanics* **32** (3), 459-468.

Dean, R.H and Hutchinson, J.W. [1980]. Quasi-static Crack Growth in Small-Scale Yielding. *ASTM STP 700*, 383-405.

Gifford, L.N. [1975]. APES-Second Generation Two-Dimensional Fracture Mechanics and Stress Analysis by Finite Elements. DTNSRDC Report 4799.

Gifford, L.N. [1978]. J-Integral Analysis of a Compact JIC Specimen. DTNSRDC Report.

Goods, S.H. and Brown, L.M. [1979]. The Nucleation of Cavities by Plastic Deformation. *Acta Metallurgica*, **27**, 1-15.

Hilton, P.D. and Gifford, L.N. [1983]. Elastic-Plastic Finite Element Analysis of Two-Dimensional Crack Problems. In: *Elastic-Plastic Fracture: 2nd Symposium ASTM STP 803* [Eds. C.F. Shih and J.P. Gudas] (Vol. I--Inelastic Crack Analysis, pp. I256-I273 ) Philadelphia: American Society for Testing and Materials.

Hutchinson, J.W. [1968]. Singular Behaviour at the End of a Tensile Crack in a Hardening Material*Journal of the Mechanics and Physics of Solids* **16**, 13-31.

Hutchinson, J.W. [1983]. Fundamentals of the Phenomenological Theory of Non-linear Fracture Mechanics. *ASME Journal of Applied Mechanics*, **50**, 1042-1051.

Jun, S. et al.[1991]. Crack-Tip Constraint and J-Controlling Stable Growth of Crack in Plane Stress Case. *Engineering Fracture Mechanics* **39** (6) 1045-1049.

McClintock, F.A. [1971]. Plasticity Aspects of Fracture; In: *Fracture: An Advanced Treastise* (volume 3, pp. 47-225) New York: Academic Press.

McMeeking, R.M. and Parks, D.M. [1979]. On Criteria for *J* Dominance of Crack Tip Fields in Large-Scale Yielding. In: *Elastic-Plastic Fracture, ASTM STP 668* [Eds. J.D. Landes, J.A. Begley, and G.A. Clarke] Philadelphia: American Society for Testing and Materials.

McMeeking, R.M. and Parks, D.M., [1979]. On Criteria for *J* Dominance of Crack Tip Fields in Large-Scale Yielding. *ASTM STP 668*, 175-194.

McMeeking, R.M. [1977]. Finite Deformation Analysis of Crack-Tip Opening in Elastic-Plastic Materials and Implications for Fracture. *Journal of the Mechanics and Physics of Solids*, **25**, 357-381.

McMeeking, R.M. [1977]. Finite Deformation Analysis of Crack-Tip Opening in Elastic-Plastic Materials and Implications for Fracture. *Journal of the Mechanics and Physics of Solids*, **25**, 357-381.





Metals Handbook volume 2, Edited by H.E. Boyer and T.L. Gall, Metals Park, OH, American Society for Metals, 1985.

Needleman, A. and Tvergaard, V. [1983]. Crack Tip Stress and Deformation in a Solid with a Vertex on its Yield Surface. *ASTM STP 803*, vol. 1, p. 803.

Needleman, A. and Tvergaard, V. [1983]. Crack Tip Stress and Deformation in a Solid with a Vertex on its Yield Surface. In: *Elastic-Plastic Fracture: 2nd Symposium ASTM STP 803* [Eds. C.F. Shih and J.P. Gudas] (Vol. I--Inelastic Crack Analysis, pp. I-80-I-115) Philadelphia: American Society for Testing and Materials.

Orowan, E. [1950]. *Fatigue and Fracture of Metals*. Cambridge: MIT press.

Rice, J.R. and Rosengren, G.F. [1968]. Plane Strain Deformation Near a Crack Tip in a Power-Law Hardening Material. *Journal of the Mechanics and Physics of Solids* **16**,1-12.

Schmitt, W. and Kienzler, R. [1989]. The *J*-Integral Concept for Elastic-Plastic Material Behavior. *Engineering Fracture Mechanics*, **32** (3), 409-418.

Schmitt, W. and Kienzler, R. [1989]. The *J*-integral Concept for Elastic-Plastic Material Behavior. *Engineering Fracture Mechanics*, **32** (3), 409-418.

Shih, C.F. and German, M.D. [1981]. Requirement for a One Parameter Characterization of Crack Tip Fields by the HRR Singularity. *Int Journal of Fracture* **17**, 27-43.

Shih, C.F. and German, M.D. [1981]. Requirement for a One Parameter Characterization of Crack Tip Fields by the HRR Singularity. *International Journal of Fracture*, **17**, 27-43.

Sorensen, E.P. [1979]. A Numerical Investigation of Stable Crack Growth Under Small Scale Yielding Conditions. *ASTM STP 668*, 151-174.

Vanderglas, M.L. [1990]. Experiences Using Three-Dimensional Finite Element Analysis for Leak-Before-Break Assessment *International Journal of Pressure Vessels & Piping*, **43**, 241-253.

Vanderglas, M.L., [1990]. Experiences Using Three-Dimensional Finite Element Analysis for Leak-Before-Break Assessment. *Int J Pres Ves & Piping* **43**, 241-253.